International Journal of Scientific Research and Engineering Development-– Volume 7 Issue 3, May-June 2024
Available at www.ijsred.com

RESEARCH ARTICLE OPEN ACCESS

The Predictive Signals for the South Indian Summer Precipitation from the Equatorial African Spring Soil Temperature

Pita Gampalage Yasarathna*, Dinesh Madhushanka**
*(School of Atmospheric Science, Nanjing University of Information Science and Technology, Nanjing, China
Email: pgrathna@outlook.com)
**(School of Applied Meteorology, Nanjing University of Information Science and Technology, Nanjing, China
Email: r.m.d.karunarathna@gmail.com)

----------**********----------

Abstract:

The South Asian Summer Monsoon (SASM) region including south India sustains millions of livelihoods with an economy primarily based on agriculture. Since about 70% of the annual precipitation occurs during the summer season from June to September, even minor precipitation fluctuations can significantly impact people's lives. Reliable seasonal predictions are crucial for managing extreme events related damages. This study aims to improve seasonal summer predictions for the South India (SI) regionby incorporating preceding spring Soil Temperature (ST). The study focuses on the SI region (8°N-19°N, 73°E-84°E) and analyzed 40 years of ERA5 data (1983-2022) from the ECMWF. South Indian Summer Precipitation (SISP) index, calculated by area averaging precipitation was employed to identify the influence of preceding spring ST on the SI. Results indicate that equatorial Africanspring ST have significant correlations with the SISP with the coefficient approximately 0.50. Then, from the analysis of other climatic factors in the spring and summer seasons, the possible mechanism for the influence of the spring ST in equatorial Africa on the SISP was identified. After that, African spring ST was used to improve the seasonal prediction skill of the Climate Forecast System version 2 (CFSv2) model for the SI region. In a statistical multiple linear regression model, applying spring ST as a variable with CFSv2, the predictive skill improved from 0.56 to 0.67. Accordingly, it is possible to use equatorial African ST to improve the seasonal prediction of SISP.

Keywords **—Seasonal Prediction, Soil Temperature, South Indian Summer Precipitation.**

----------**********----------

I. INTRODUCTION

The monsoon affects two-thirds of the world's population as well as a large portion of the planet's surface [1], and its main climate patterns are experienced in tropical regions and the SASM is one of the most robust monsoon systems, contributing more than 70% to the annual precipitation in the Indian subcontinent [2], [3]. The SASM is characterized by the south-westerly wind flow to the land that brings moisture from the Indian Ocean to the Indian subcontinent during the summer monsoon period of JJAS (June to September)[4]. Even though the inter-annual variation is about 10% of the SASM precipitation total [5], this inter-annual variation of the long-term seasonal mean precipitation over the Indian region is strongly correlated with food production, and the extremes in year-to-year variations of the long-term mean precipitation manifest large-scale floods and droughts [6]. It is one of the region's most significant climate phenomena and profoundly impacts agriculture, irrigation, water resources, hydropower, transportation, and overall livelihoods [7]. The Indian economy is also very closely linked with the variability of the SASM [8].

Generally, the SASM commencement occurred the last week of May in Kerala in Indian mainland [9] and Andaman Island in the Bay of Bengal, Sri Lanka, etc. After that, the rainy belt advances from the southern to the northern parts of India during June. It fully covers the Indian subcontinent in July and gradually withdraws to the south in September [10]. Although the SASM rainy season lasts from

June to September, there are also rainy and non-rainy (active and break) monsoon seasons during that period [11], and it happens according to the change in low-level jet (LLJ) strength, atmospheric circulations, etc. Precipitation distribution varies across and within countries due to spatial topography, location and other natural factors in the region. The western part of the SI and the northeastern of the SASM region receive the most precipitation, while the northwestern region receives less [4], and the average precipitation is about 8mm per day [12]. The SASM is heavily affected by both annual variations and inter-seasonal variations. Even minor shifts in the intensity or timing of seasonal rains can have a substantial impact on the millions of people who live in the region [13]. Floods and droughts are common in this region due to such extreme events.

The highest concentration of rain-fed agriculture occurs in western and southern areas of India under oilseed, grain, and cotton cultivation and in the east, where much of the rice is rain fed [14]. The SASM precipitation is critical to the 'kharif' crop, which contributes over 50% of India's food-grain production and 65% of its oilseeds production. Annual fluctuations in summer precipitation significantly affect the overall kharif food-grain production [14], [15]. The 'rabi' growing season, starting in autumn and extending to spring, relies on post-monsoon precipitation for soil moisture and irrigation. Thus, summer precipitation supports both kharif and rabi crop production over India [14].

The Indian Summer Monsoon or the SASM precipitation variability is governed by the Eastern and Central Pacific El Niño Southern Oscillation (ENSO), equatorial zonal winds, Atlantic zonal mode, and surface temperatures of the Arabian Sea and the Bay of Bengal [4]. The ENSO-related SST variabilities in the equatorial Pacific Ocean are coupled to the atmospheric Walker circulation [11]. During the El Nino conditions, the overall Walker circulation is where the descending branch of the Walker cell in the western Indian Ocean shifts eastward over the Indian subcontinent, resulting in reduced convection. In the La Nina situation, the entire Walker cell slightly shifts westward, strengthening convection across the Indian subcontinent [2]. As a result of the Walker circulation's fluctuations, El Nino events tend to suppress precipitation, and the La Nina events tend to enhance the SASM precipitation [12], [16]. So, the typical pattern of decreased rainfall during El Nino years and increased rainfall during La Nina years [4], [16]. However, over the previous 40 years, the relationship between ENSO and the SASM monsoonal rainfall has stayed consistent when accounting for the length of the monsoon [17]. Through the equatorial Rossby wave response and the anomalous Walker circulation, a developing La Nina event is typically linked to delayed termination and an earlier beginning, resulting in a prolonged Asia summer monsoon (including SASM) length [17].

Most positive IOD events correspond with positive anomalies in the concurrent SASM. Similarly, negative IOD events correspond with negative anomalies in the SASM precipitation [2], [4], [16], [18]. Also, the IOD plays a vital role as a modulator in the Indian region monsoon precipitation and influences the correlation between the SASM and ENSO. The IOD and the ENSO have complementarily affected the SASM precipitation during the last four decades. During El Nino with a positive IOD, the SASM rainfall shows a positive anomaly due to favorable conditions for convective processes in the Bay of Bengal region. On the other hand, although La Nina increased SASM precipitation, the presence of La Nina with a negative IOD causes SASM to show a negative anomaly [2], [18].

The effect of SST has been much investigated due to the large heat capacity of ocean water, which is approximately three times higher than that of soil, and the significant horizontal transport of heat [19]. In addition, land-atmosphere interactions are also essential factors in improving the reliability of climate predictions [20], [21], and the ST (as well as soil moisture) play an immense role in land-atmosphere interaction. According to recent studies, pre-monsoonal land temperature conditions may have a greater impact on the SASM precipitation in early summer than in late summer [10]. In another sample by Wu & Zhang (2014), the subsurface ST feedback influences summer precipitation and the surface air temperature in East Asia. The subsurface ST memory typically persists for about 3- 15

months in arid and the semiarid regions and persists in non-arid regions for up to 3 months [22].

Land-atmosphere interaction involves complex interactions between various variables. The feedback mechanisms further complicate this due to their inter-connectedness. When considering the physical processes involved in the water and energy balance, all the variables are interconnected and ranked according to the magnitude of their influence [23]. In general, ST represents the soil energy status and heat transfer conditions [24]. Also, the ST affects the surface temperature and creates a temperature gradient between the surface and the lower atmosphere [19]. It affects climate through atmospheric circulation by influencing surface energy and water budgets [22]. In general, heat is transferred to deep soil layers and stored in the warm seasons, and that energy is released upward in cold seasons, thereby increasing the surface ST [22], [24]. So, the ST represents soil energy status, heat storage, and heat transfer conditions [19], [25], [26]. The variation in ST was closely related to soil water content, which can change soil heat capacity and thermal conductivity [27]. According to Hu and Feng's (2004), the soil enthalpy anomaly in the top 1m soil column could persist for about 2-3 months. The ST may incorporate an extended memory element, potentially enhancing predictability [19]. Thus, the sensible heat flux is affected. Generally, the ST is an important parameter for evaluating soil thermal properties and can be used to calculate and predict the net heat entering the surface energy balance [27].

Global Climate Models (GCMs) typically operate at low resolution 100 km to 300 km, capturing large scale global systems. They struggle to accurately depict small-scale features like land cover, topography, and atmospheric dynamics, which limits their ability to predict small scale extreme weather and climate events accurately [28]. Hence, Regional Climate Models (RCMs) are employed for dynamical downscaling to derive regional or local climate information from GCMs. Typically, RCMs operates at a 50km, but recently, higher resolution RCMs have become common, especially when detailed climate information is needed [29]. When RCM simulated with air-sea interaction taken into account, notable enhancements in monsoon circulation, precipitation, and intra-seasonal variability are observed [28], [30].

Historically, seasonal predicts for SASM precipitation have used statistical methods. However, the growing demand for climate services requires integrating skilled seasonal predictions from various modelling centres to generate objective climate outlooks [12]. Improved SASM predicting can alleviate water stress for agriculture and domestic needs and mitigate the impacts of hydrometeorological disasters [31]. The South Asia Seasonal Climate Outlook Forum (SASCOF) issues seasonal predictions for the SASM region using 12 dynamical models [12]. According to Stacy et. al., (2023), while SASCOFs seasonal predictions show significant skill in some areas of the SASM region, there is still a need for further improvement.

Therefore, the main objective of this study is to investigate whether the interannual variability of SISP is influenced by preceding spring ST, and whether it can provide any signal about the coming summer monsoon precipitation. The data and methodology are described in section II. The results and discussion provided in section III. The conclusions are presented in section IV.

II. DATA AND METHOD

A. Data

For this study, reanalysis data such as precipitation, soil temperature, wind and sea surface temperature for a 40-year period from 1983 to 2022 are used, which are monthly data from the European Centre for the Medium-Range Advanced Atmospheric Reanalysis v5 (ERA5) dataset, Retrieved from Weather Forecast (ECMWF). The ERA5 is the fifth generation ECMWF atmospheric global climate reanalysis, covering the period from January 1940 to date.

Also, the Climate Forecast System version 2 (CFSv2) model monthly rainfall data was also used for the above 40 years. The CFSv2 monthly precipitation data, produced by the National Centre for Environmental Prediction (NCEP), have been used to improve and compare the multi-linear regression model predictions (noaa.gov). The complete details about the data used for the study are summarized in the table (Table 1).

Table 1. Details of the data which are used for the study. All the data is downloaded monthly.

Data element	Level	Units	From	Resolution
Meridional wind	850 hPa	ms^{-1}	ECMWF , ERA5	0.25° x 0.25°
Meridional wind	200 hPa	ms^{-1}	-do-	-do-
Zonal wind	850 hPa	ms^{-1}	-do-	-do-
Zonal wind	200 hPa	ms^{-1}	-do-	-do-
Soil Temperature (Layer 1)	0-7 cm	K	-do-	-do-
Precipitation	Surface	m	-do-	-do-
Precipitation	Surface	m	NOAA, CFSv2	1° x 1°

B. Method

The monsoon indices employed by various researchers, primarily about the SASM, were considered. The Extended Indian Monsoon Rainfall (EIMR) index is defined as the summer monsoon precipitation averaged over the region of 10° N to 30° N latitude and 70° E to 110° E longitude [32]. This EIMR index covers an area that extends beyond the Indian land area. When a large area is selected, and an area-averaged index is prepared using this method, the accuracy of the index may be reduced. Therefore, the SI region (08° N to 19° N, 73° E to 84° E) was selected as the plotted region by the yellow-coloured box (Fig. 1). The selected SISP region includes four provinces of India, which are Karnataka, Andra Pradesh, Kerala and Tamil Nadu.

The SISP index was obtained for the plotted region by area average precipitation for the summer season was calculated by summing the area average for 4 months of JJAS in the region selected as the SISP region. Also, the area average anomaly of the spring ST was used as the ST index for the correlations study.

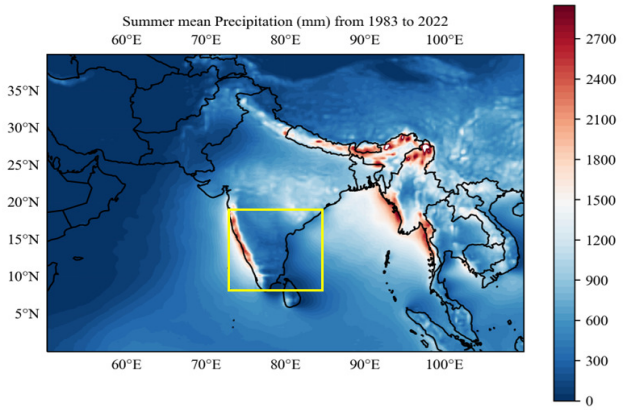

Fig. 1 The summer season (JJAS) average precipitation (mm) for 40 years from 1983 to 2022, was analysed using ECMWF ERA5 reanalysis data. The study region 'SISP' is marked with a yellow box.

This study used Pearson's correlation coefficient to calculate the correlation between each variable. Also, the linear correlation between each variable was tested in multiple instances. The student's t-test for significance was performed in each of these instances, with a significance level kept at 5% for accuracy. A multi-linear regression model has been used for the SISP prediction using spring ST and CFSv2 model data as predictors.

III. RESULTS AND DISCUSSION

A. Spring ST Influence on the SISP

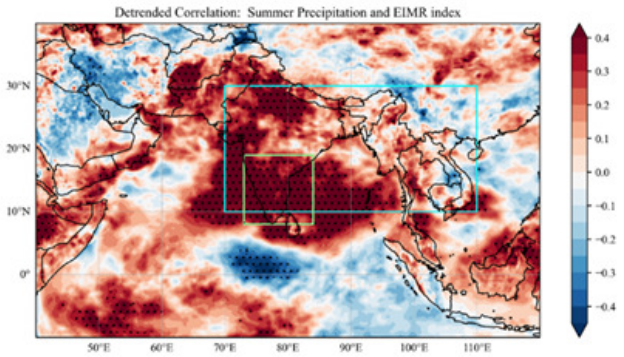

Fig. 2 Detrended correlation between the summer precipitation and EIMR index. The EIMR and SISP regions are marked with cyan and light-green coloured boxes, respectively.

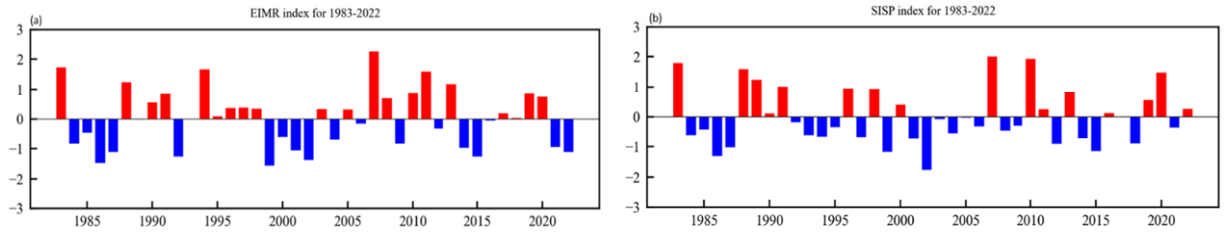

Fig. 3(a) The EIMR (10° N to 30° N and 70° E to 110° E) index (b) Southern India (8° N to 19° N and 73° E to 84° E) summer precipitation index.

The long-term detrended correlation between the summer precipitation and the EIMR index is shown in Fig. 2. Also, the EIMR and SI regions are marked with cyan and light green boxes, respectively, on the map. Both EIMR and SISP indices (Fig. 3) were calculated by looking for anomalies in the average summer precipitation for the regions corresponding to each index, respectively as defined earlier. The correlation coefficient between the EIMR and SISP indices was about 0.71.

The correlations map indicates how the SISP is influenced by regional spring ST. Spring ST over equatorial Africa was found to have a significant positive correlation with the SISP index (Fig. 4). The regions that were identified encompassed the areas inside 14° S to 9° N and 14° E to 39° E over equatorial Africa, as depicted in figure with the green coloured boxes. The dotted areas are statistically significant at the 5% level based on the student's t-test.

After identifying the regions of spring ST that correlated with the SISP index, the area index was calculated for that region.Accordingly, the resulting area index represents the average anomalies of boreal springtime ST conditions over equatorial Africa.

Then, the long-term detrended ST area index was plotted alongside the annual variations in the SISP index (Fig. 5). The dotted green line depicts the detrended precipitation index of the SI region. This detrended index is created by removing long-term trends from a dataset. This allows for a clearer analysis of the year-to-year variations in the series.Then the correlation coefficients between the detrended normalized equatorial Africa's Spring ST indices and the SISP index remained 0.50.

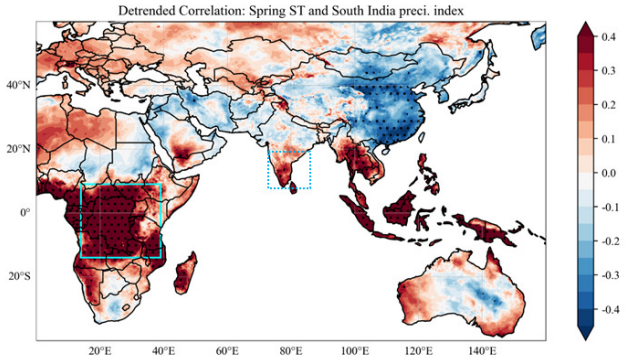

Fig. 4 The detrended correlation between the spring ST and the SISP index. The significantly correlated region, according to the 5% level student t-test, is marked with a light-blue box,

Based on the previously mentioned results, it has been confirmed that a statistically significant correlation exists between Africa preceding spring ST and SISP index. Fig. 6 visually represent the correlation of Africa Spring ST with the SISP and the selected SI region marked by a light blue box on map. In the map, the long-term trend has been removed, and the 5% level of statistically significant areas is shown by dotted.

The equatorial Africa Spring ST correlation influences the SI region, particularly in southern and western coastal areas of the Indian subcontinent. However, it shows a weak correlation with the northern and northeastern parts of India and over the north Bay of Bengal region. This weak

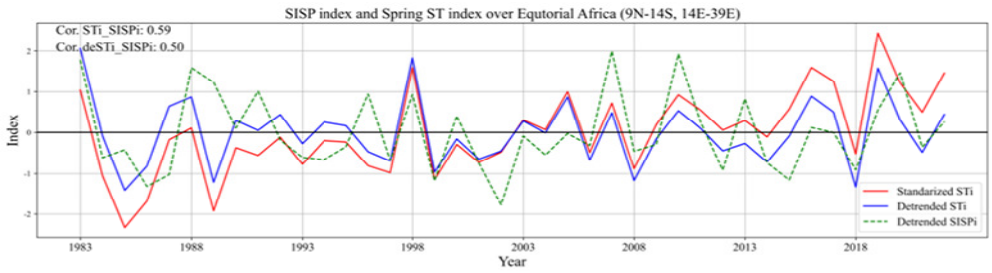

Fig. 5 The SISP index with the trended and detrended spring ST indices over the equatorial Africa

correlation is likely due to the presence of the Western Ghats Mountain range along the western coastal region of India, which blocks the spread of the ST effects to the eastern and northern regions.

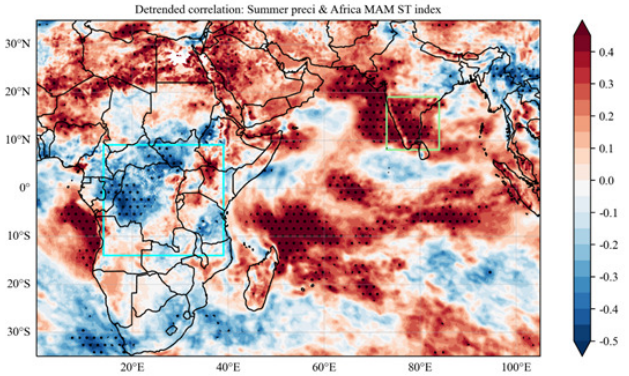

Fig. 6 The detrended correlation between summer precipitation and equatorial Africa boreal spring ST index. The dotted areas are statistically significant at the 5% level based on the student's t-test.

B. Possible Physical Mechanism

In the identified area of equatorial Africa (14° S to 9° N and 14° E to 39° E), the Northern Hemisphere is in the spring season (boreal spring), a period when the sun's energy is at its maximum. Because the sun is overhead in the equatorial African region as it migrates from south to north, anomalous solar radiation reaches the region during the boreal spring season. Also, it is the first rainy season in equatorial Africa [33], [34], [35]. As a result of these two occurrences during the same period, the capacity to store thermal energy in the soil increases due to wet soil's ability to absorb more energy. Because of the memory of the soil temperature for about 2-3 months [19], it persists until the following summer (Figure 7).

The soil surface becomes hotter than the atmosphere due to the warm and wet soil in the summer. The heat energy is then transferred through the surface layer into the inner soil layers, increasing the ST in the region. In addition, the region sees an increase in convective rain during the spring [33]. As a result, the evapotranspiration process is enhanced by land-atmosphere temperature contrast. The local low-level atmosphere becomes a favorable upward motion and develops circulation.

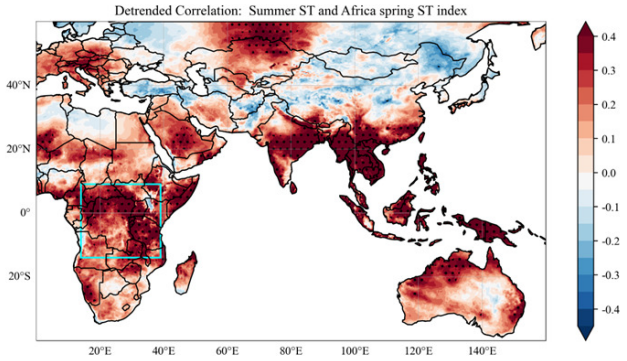

Fig. 7 The Detrendedcorrelation between Summer ST and Spring ST index over equatorial Africa.The dotted areas are statistically significant at the 5% level based on the student's t-test.

Furthermore, the regional middle and upper levels block upward motion by influencing sinking motions or strong subsidence over the vicinity of the North African desserts [15]. The local circulation turned eastward, further strengthening the westerly (Figure 9a), the LLJ flow over the Arabian Sea. And then it reinforced the SISP. Now, let us try to clarify that situation through results. Additionally, as shown in Figure 8, the correlation coefficient between the two indices of the SISP and Africa ST area index was 0.50, which was statistically significant at the 5% level based on the student's t-test.

Furthermore, Fig. 7 and Fig. 8 show a significant correlation between the summer ST and spring ST area indices over the equatorial Africa region, with a correlation coefficient of about 0.39. Accordingly, spring and summer ST may be correlated due to the memory of 2-3 months in ST. Thus, during summer, evapotranspiration increases due to the high soil surface temperature, which is favourable for forming atmosphere circulations.

The correlation with the spring ST index in the equatorial Africa region with 850 hPa and 200 hPa winds in the summer, the SI region, and the equatorial Africa region is marked (as the cyan-coloured box) in those two maps (Fig. 9).

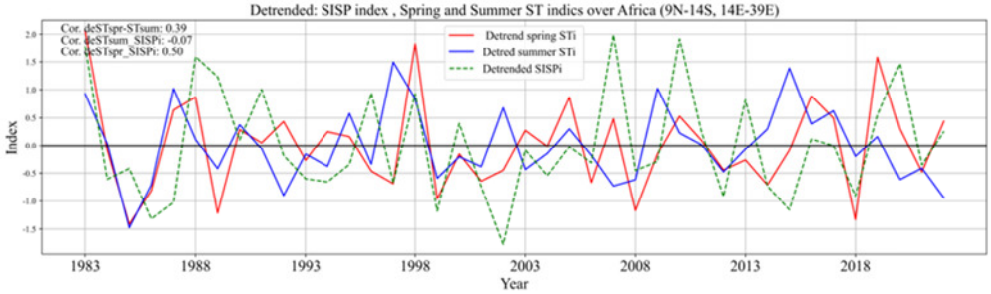

Fig. 8 Correlation between detrended SISP index, summer ST and spring ST indices over Africa.

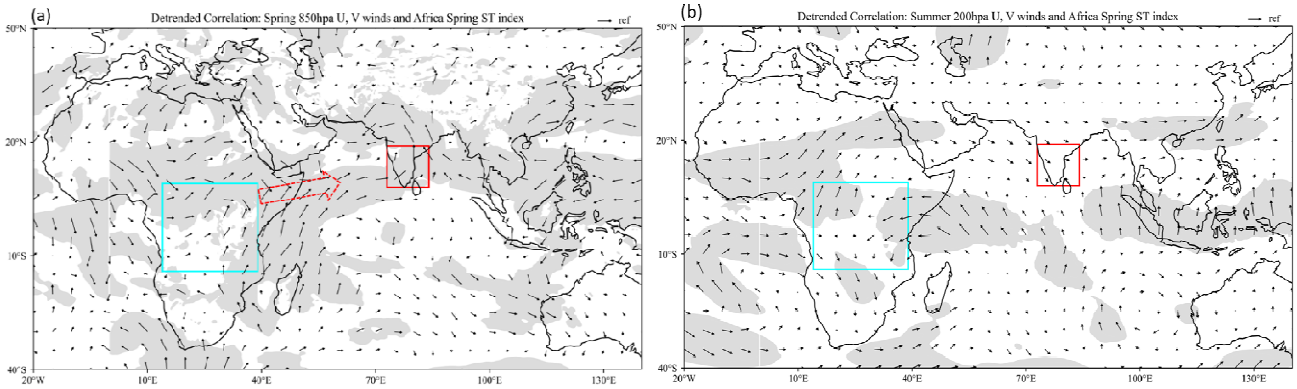

Fig. 9 Detrended correlation between Africa Spring ST area index and summer U, V winds at (a) 850 hPa & (b). 200 hPa. The shaded areas are statistically significant at the 5% level based on the student's t-test.

Considering summer 850 hPa, an equatorial Africa region shows winds blowing into the SASM across the Arabian Ocean and a circulation over west and northwest India. The African region's flow has the potential further to enhance the westerly LLJ. The upper level (or 200 hPa) winds show a divergence (or mild anti-cyclonic circulation) over the northwestern part of India, which might be associated with the low-level cyclonic circulation inthe 850 hPa correlation map.

Accordingly, the influence of the spring ST in equatorial Africa results in an increase in SISP intensity. Considering the correlation map between Africa Spring ST and summer 850 hPa winds in Figure 9a, although the winds reached the Indian landmass from the west through the Arabian Sea, they did not travel to the east of India and the Bay of Bengal, and a cyclonic circulation has occurred in the west of India. It may be due to the influence of the western Ghats Mountain range in that region of India. The flow chart schematically shows this possible process of equatorial Africa Spring ST influence on SISP (Fig. 10).

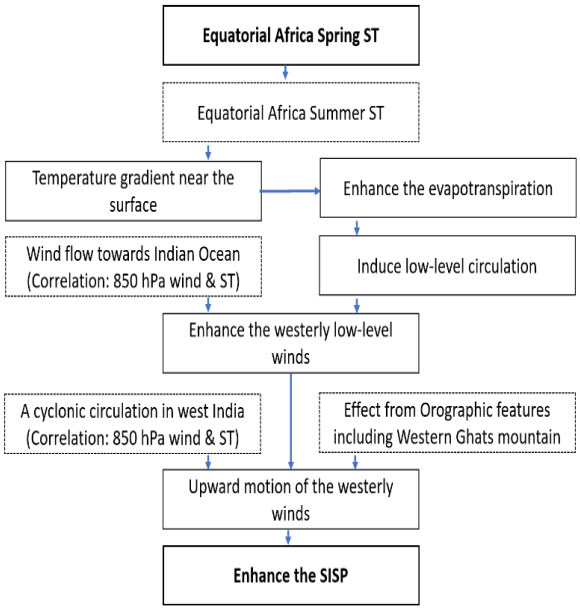

Fig. 10 The possible mechanism for equatorial Africa Spring ST influence on the Sout India summer precipitation

C. Seasonal Prediction

In this study, the 40-year ERA5 reanalysis monthly precipitation data from 1983 to 2022 are

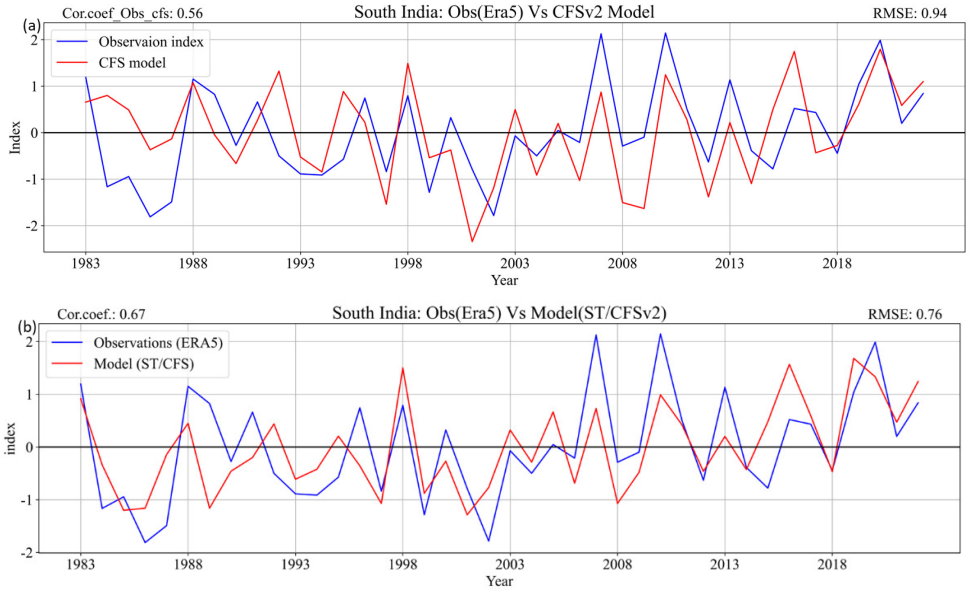

Fig. 11 South Indian Region's annual summer monsoon precipitation variation. Observation and (a) CFSv2 model, (b) the multi-linear regression model using spring ST and the CFSv2 data

considered observation data for the performing SISP index. Amulti-linear regression model can be written using the following equation:

$$Y = aX_1 + bX_2 + c$$

An input feature matrix, 'X' was initially created with two factors or features. Subsequently, the target variable matrix, 'Y' was formulated using the above equation. The coefficients of 'a' and 'b' represent the factors, and 'c' represents the intercept in the formula. The model yielded values for these coefficients. Then, the target variable matrix Y contains the corresponding values for the target variable.

Using the above-identified equatorial Africa Spring ST and the CFSv2 model data, the prediction skill of the SISP was investigated for the study period 1983 to 2022. It is shown that the prediction skill of CFSv2 model data for SI region is about 0.56 (Figure 11a). When a multi-linear regression model was used using the CFSv2 model data with the identified Africa Spring ST values as features, the prediction skill could be increased to 0.67, as shown in the Figure 11b. A study using a combined spring ST and CFSv2 model data for the 40-year period shows improved prediction accuracy in most years. This approach also reduced the tendency of the CFSv2 model to overestimate or underestimated flow rates.

IV. CONCLUSIONS

Analysis of the SISP index with equatorial African spring ST revealed a significant correlation and the correlation coefficient is about 0.50 at the 5% significance level using a student's t-test. The study examined possible mechanisms to understand the influence of spring ST on SISP. Various climatological parameters were considered, including summer and spring seasons SST, low-level winds, upper-level winds, etc. Through the analysis of these correlations and the insights from previous studies, helped explain the underlying mechanism.

The correlation coefficient between the observations and the CFSv2 dynamic model predictions for the SI region over the 40-year study period is about 0.56 indicating significant prediction skill. When the multi-linear regression model is used with the CFSv2 model data and the Africa Spring ST variables, the prediction exhibits a significant level of skill reaching approximately 0.67. The proposed model using spring ST with CFSv2 shows better proficiency in extreme event detection as well as seasonal prediction.Also, when

the CFSv2 model data is used with Africa Spring ST, the error of the seasonal prediction is reduced from 0.94 to 0.76.

Based on the above finding, signals related to the seasonal variability of the SISP can be obtained by ST during the preceding spring season in equatorial Africa. Accordingly, leveraging the Spring ST data available by the end of May, it becomes feasible to develop a model forecast. The CFSv2 model prediction can be improved by using the equatorial African spring ST variable at the beginning of June, when SISP begins, thereby supporting water management and managing the potential impacts of extreme events in the region.

ACKNOWLEDGMENT

I would like to express my special gratitude to School of Atmospheric Science, Nanjing University of Information Science and Technology for providing the opportunity for this study. Also, I would like to sincerely thanks to my supervisor, Ass. Prof. Huang Yanyan for her invaluable guidance, unwavering support and mentorship throughout this study. Her expertise, encouragement, and constructive feedback have been instrumental in shaping the direction of this study and pushing me to achieve my best. I am deeply grateful to senior colleague Mr. Qian Danwei, for his generous assistance and technical expertise. Finally, I would like to express my gratitude to all my friends, who have helped and encouraged me in making this success.

REFERENCES

[1] B. Wang et al., "Monsoons climate change assessment," Bull Am Meteorol Soc, vol. 102, no. 1, pp. E1–E19, Jan. 2021, doi: 10.1175/BAMS-D-19-0335.1.

[2] P. K. Pothapakula, C. Primo, S. Sørland, and B. Ahrens, "The synergistic impact of ENSO and IOD on Indian summer monsoon rainfall in observations and climate simulations-an information theory perspective," Earth System Dynamics, vol. 11, no. 4, pp. 903 – 923, Nov. 2020, doi: 10.5194/esd-11-903-2020.

[3] Yadav M, "Disaster Resilience and Green Growth Series Editors," 2022.doi:10.1007/978-981-16-7727-4

[4] P. J. Nair, A. Chakraborty, H. Varikoden, P. A. Francis, and J. Kuttippurath, "The local and global climate forcings induced inhomogeneity of Indian rainfall," Sci Rep, vol. 8, no. 1, Dec. 2018, doi: 10.1038/s41598-018-24021-x.

[5] A. G. Turner and H. Annamalai, "Climate change and the South Asian summer monsoon," Nature Climate Change, vol. 2, no. 8. pp. 587–595, Aug. 2012. doi: 10.1038/nclimate1495.

[6] B. N. Goswami and Lau W, "South Asian monsoon," in Intraseasonal Variability in the Atmosphere-Ocean Climate System, Springer Berlin Heidelberg, 2007, pp. 19–61. doi: 10.1007/3-540-27250-x_2.

[7] X. Zeng and E. R. Lu, "NOTES AND CORRESPONDENCE Globally Unified Monsoon Onset and Retreat Indexes," 2004.https://iri.columbia.edu/~ousmane/print/Onset/ZengLu04_JClim.pdf

[8] Mooley D. and Parthasarathy B., "Variability of the Indian Summer Monsoon and Tropical Circulation Features," 1983.https://doi.org/10.1175/1520-493(1983)111<0967:VOTISM>2.0.CO;2

[9] P. N. Preenu, P. V. Joseph, and P. K. Dineshkumar, "Variability of the date of monsoon onset over Kerala (India) of the period 1870–2014 and its relation to sea surface temperature," Journal of Earth System Science, vol. 126, no. 5, Jul. 2017, doi: 10.1007/s12040-017-0852-9.

[10] J. Yang and H. Chen, "Influences of Spring Land Surface Thermal Anomalies over West Asia on Indian Early Summer Monsoon Activity and Its Pathway," J Clim, vol. 35, no. 18, pp. 6051–6074, Sep. 2022, doi: 10.1175/JCLI-D-21-0916.1.

[11] S. Gadgil, "The Indian monsoon and its variability," Annu Rev Earth Planet Sci, vol. 31, pp. 429–467, 2003, doi: 10.1146/annurev.earth.31.100901.141251.

[12] J. Stacey et al., "Diverse skill of seasonal dynamical models in forecasting South Asian monsoon precipitation and the influence of ENSO and IOD," Clim Dyn, vol. 61, no. 7–8, pp. 3857–3874, Oct. 2023, doi: 10.1007/s00382-023-06770-2.

[13] H. Yang, K. R. Johnson, M. L. Griffiths, and K. Yoshimura, "Interannual controls on oxygen isotope variability in Asian monsoon precipitation and implications for paleoclimate reconstructions," J Geophys Res, vol. 121, no. 14, pp. 8410–8428, 2016, doi: 10.1002/2015JD024683.

[14] K. Krishna Kumar, K. Rupa Kumar, R. G. Ashrit, N. R. Deshpande, and J. W. Hansen, "Climate impacts on Indian agriculture," International Journal of Climatology, vol. 24, no. 11, pp. 1375–1393, Sep. 2004, doi: 10.1002/joc.1081.

[15] P. J. Webster et al., "Monsoons: processes, predictability, and the prospects for prediction," J Geophys Res Oceans, vol. 103, no. C7, pp. 14451–14510, Jun. 1998, doi: 10.1029/97jc02719.

[16] P. J. Webster and S. Yang, "Monsoon and Enso: Selectively Interactive Systems," Quarterly Journal of the Royal Meteorological Society, vol. 118, no. 507, pp. 877–926, 1992, doi: 10.1002/qj.49711850705.

[17] P. Hu, W. Chen, L. Wang, S. Chen, Y. Liu, and L. Chen, "Revisiting the ENSO-monsoonal rainfall relationship: new insights based on an objective determination of the Asian summer monsoon duration," Environmental Research Letters, vol. 17, no. 10, Oct. 2022, doi: 10.1088/1748-9326/ac97ad.

[18] K. Ashok, Z. Guan, and T. Yamagata, "Impact of the Indian Ocean dipole on the relationship between the Indian monsoon rainfall and ENSO," Geophys Res Lett, vol. 28, no. 23, pp. 4499–4502, Dec. 2001, doi: 10.1029/2001GL013294.

[19] Y. Xue, R. Vasic, Z. Janjic, Y. M. Liu, and P. C. Chu, "The impact of spring subsurface soil temperature anomaly in the western U.S. on North American summer precipitation: A case study using regional climate model downscaling," Journal of Geophysical Research Atmospheres, vol. 117, no. 11, 2012, doi: 10.1029/2012JD017692.

[20] C. Gao et al., "Land–atmosphere interaction over the Indo-China Peninsula during spring and its effect on the following summer climate over the Yangtze River basin," Clim Dyn, vol. 53, no. 9–10, pp. 6181–6198, Nov. 2019, doi: 10.1007/s00382-019-04922-x.

[21] M. Li, P. Wu, and Z. Ma, "A comprehensive evaluation of soil moisture and soil temperature from third-generation atmospheric and land reanalysis data sets," International Journal of Climatology, vol. 40, no. 13, pp. 5744–5766, Nov. 2020, doi: 10.1002/joc.6549.

[22] L. Wu and J. Zhang, "Strong subsurface soil temperature feedbacks on summer climate variability over the arid/semi-arid regions of East Asia," Atmospheric Science Letters, vol. 15, no. 4, pp. 307–313, Oct. 2014, doi: 10.1002/asl2.504.

[23] K. L. Brubaker and D. Entekhabi, "Analysis of feedback mechanisms in land-atmosphere interaction," Water Resour Res, vol. 32, no. 5, pp. 1343–1357, May 1996, doi: 10.1029/96WR00005.

[24] C. Zhao, H. Chen, and S. Sun, "Evaluating the Capabilities of Soil Enthalpy, Soil Moisture and Soil Temperature in Predicting Seasonal

Precipitation," Adv Atmos Sci, vol. 35, no. 4, pp. 445–456, Apr. 2018, doi: 10.1007/s00376-017-7006-5.

[25] S. P. P. Mahanama, R. D. Koster, R. H. Reichle, and M. J. Suarez, "Impact of subsurface temperature variability on surface air temperature variability: An AGCM study," J Hydrometeorol, vol. 9, no. 4, pp. 804–815, 2008, doi: 10.1175/2008JHM949.1.

[26] X. Fang, S. Luo, and S. Lyu, "Observed soil temperature trends associated with climate change in the Tibetan Plateau, 1960–2014," Theor Appl Climatol, vol. 135, no. 1–2, pp. 169–181, Jan. 2019, doi: 10.1007/s00704-017-2337-9.

[27] X. Chen et al., "The spatiotemporal variations of soil water content and soil temperature and the influences of precipitation and air temperature at the daily, monthly, and annual timescales in China," Theor Appl Climatol, vol. 140, no. 1–2, pp. 429–451, Apr. 2020, doi: 10.1007/s00704-020-03092-9.

[28] Z. Xu, Y. Han, and Z. Yang, "Dynamical downscaling of regional climate: A review of methods and limitations," Science China Earth Sciences, vol. 62, no. 2. Science in China Press, pp. 365–375, Feb. 01, 2019. doi: 10.1007/s11430-018-9261-5.

[29] J. Karmacharya, R. Jones, W. Moufouma-Okia, and M. New, "Evaluation of the added value of a high-resolution regional climate model simulation of the South Asian summer monsoon climatology," International Journal of Climatology, vol. 37, no. 9, pp. 3630–3643, Jul. 2017, doi: 10.1002/joc.4944.

[30] J. V. Ratnam, F. Giorgi, A. Kaginalkar, and S. Cozzini, "Simulation of the Indian monsoon using the RegCM3-ROMS regional coupled model," Clim Dyn, vol. 33, no. 1, pp. 119–139, 2009, doi: 10.1007/s00382-008-0433-3.

[31] A. Chevuturi et al., "Forecast skill of the Indian monsoon and its onset in the ECMWF seasonal forecasting system 5 (SEAS5)," Clim Dyn, vol. 56, no. 9–10, pp. 2941–2957, May 2021, doi: 10.1007/s00382-020-05624-5.

[32] B. N. Goswami, V. Krishnamurthy, and H. Annmalai, "A broad‐scale circulation index for the interannual variability of the Indian summer monsoon," Quarterly Journal of the Royal Meteorological Society, vol. 125, no. 554, pp. 611–633, Jan. 1999, doi: 10.1002/qj.49712555412.

[33] P. I. Palmer et al., "Drivers and impacts of Eastern African rainfall variability," Nature Reviews Earth and Environment, vol. 4, no. 4. Springer Nature, pp. 254–270, Apr. 01, 2023. doi: 10.1038/s43017-023-00397-x.

[34] X. Y. Wang et al., "Weakened seasonality of the African rainforest precipitation in boreal winter and spring driven by tropical SST variabilities," Geosci Lett, vol. 8, no. 1, Dec. 2021, doi: 10.1186/s40562-021-00192-w.

[35] S. E. Nicholson, "The ITCZ and the seasonal cycle over equatorial Africa," Bull Am Meteorol Soc, vol. 99, no. 2, pp. 337–348, Feb. 2018, doi: 10.1175/BAMS-D-16-0287.1.

